

# Matching characteristic codes: exploiting two directions

Luis Lehner

Center for Relativity, The University of Texas at Austin  
Austin, TX 78712, USA.

Combining incoming and outgoing characteristic formulations can provide numerical relativists with a natural implementation of Einstein's equations that better exploits the causal properties of the spacetime and gives access to both null infinity and the interior region simultaneously (assuming the foliation is free of caustics and crossovers). We discuss how this combination can be performed and illustrate its behavior in the Einstein-Klein-Gordon field in 1D.

## I. INTRODUCTION

In recent years the characteristic formulation of G.R. [1,2] has proven to be a valuable tool for numerical relativists\*. Its use has enabled researchers to: study critical phenomena [4,5]; obtain the first 'unlimited' evolutions of generic single black holes [6,7]; study accretion of matter by black holes [8,9] (via a formulation based on foliating the spacetime with incoming null hypersurfaces) and obtain practical access to future null infinity where the gravitational radiation and other physically relevant quantities are obtained unambiguously [10,11] (via an outgoing null hypersurfaces foliation). These investigations adopted either an outgoing or an incoming null hypersurfaces foliation of the spacetime. Regrettably, in choosing one or the other one has access to future null infinity or to the black hole interior (as the incoming null surfaces can penetrate it but not the outgoing!) but not both. This, could be regarded as a drawback for the formulation as it is desirable in many cases to access both regions; for instance, to describe a black hole accreting mass from its surrounding and the gravitational waves produced in the system.

At present, obtaining a model capable of addressing both problems at the same time requires using Cauchy-characteristic matching (CcM) [11–13] or the conformal formulation of Einstein's equations [14–16]. Unfortunately, despite much progress in both approaches neither of them is fully working in 3D. The main problem facing the CcM approach is the involved set of interpolations back and forth from a 3D cartesian grid to 2-spheres at the matching worldtube. On the other hand, the conformal approach has as a drawback its large number of variables which imposes further constraints on present computer capabilities.

The characteristic formulation [1,2], on the other hand, employs a minimum set of variables (6 compared with 12 in the ADM equations or 53 in the conformal equations). The success obtained with it in both formulations suggests that a combination of both could well be a natural way to study both regions. This approach, which we call "characteristic-characteristic matching" ( $c^2M$ ) divides the spacetime in two regions. The inner region (inside some worldtube  $\Gamma$ ) to be studied by an incoming characteristic formulation and the outer region where an outgoing formulation will be used. Interpolations are carried out at  $\Gamma$ , however in 3D it only involves two-dimensional interpolations. In a related approach, the *double null formulation* [17], Einstein equations are also integrated along incoming and outgoing null hypersurfaces and its implementation might display similar stability properties as well. Unfortunately, to date, there are no numerical implementations of this approach in 3D but studies on how to carry out such a task are under development [18]. Naturally, neither of these approaches is expected to be applicable to all situations since, for instance, the presence of caustics prevents one to use them. However, in a caustic-free foliation<sup>†</sup>,  $c^2M$  represents an enticing proposal in light of the successful application of the characteristic formulation both in the vacuum and matter cases.

We briefly describe the characteristic formulation (both in the incoming and outgoing formulation) in section 2. Section 3 outlines the matching strategy to be used in this work. We describe the numerical implementation in section 4 and test it in section 5. Finally we conclude with some comments and future research directions.

## II. THE CHARACTERISTIC FORMULATION OF G.R.

Einstein's equations can be expressed in notational form as  $G_{ab} = 8\pi T_{ab}$ . Where  $G_{ab}$  is the Einstein tensor and  $T_{ab}$  the stress energy tensor of the matter distribution. In the particular case of a massless scalar field  $\Phi$  coupled to G.R.,  $T_{ab}$  results [19]

---

\*For a recent review on its use in numerical relativity see [3].

<sup>†</sup>Aside from the natural caustic present at the origin of the null cones used to coordinatize the incoming null surfaces.

$$T_{ab} = \nabla_a \Phi \nabla_b \Phi - 1/2 g_{ab} \nabla_c \Phi \nabla^c \Phi. \quad (2.1)$$

We introduce a coordinate system adapted to either incoming or outgoing null hypersurfaces in the following way: the outgoing (incoming) lightlike hypersurfaces are labeled with a parameter  $u$  ( $v$ ); each null ray on a specific hypersurface is labeled with  $x^A$  ( $A = 2, 3$ ) and  $r$  is introduced as a surface area coordinate (i.e. surfaces at  $r = \text{const}$  have area  $4\pi r^2$ ) (see Fig. 1). In the resulting  $x^a = (u(v), r, x^A)$  coordinates, the metric takes the Bondi-Sachs form [1,2]

$$ds^2 = - (e^{2\beta} V/r - r^2 h_{AB} U^A U^B) du^2 - 2e^{2\beta} dudr - 2r^2 h_{AB} U^B dudx^A + r^2 h_{AB} dx^A dx^B, \quad (2.2)$$

for the outgoing case, while for the incoming case:

$$ds^2 = (e^{2\beta} V/r - r^2 h_{AB} U^A U^B) dv^2 + 2e^{2\beta} dudv - 2r^2 h_{AB} U^B dudx^A + r^2 h_{AB} dx^A dx^B, \quad (2.3)$$

where in both line elements,  $h^{AB} h_{BC} = \delta_C^A$  and  $\det(h_{AB}) = \det(q_{AB})$ , with  $q_{AB}$  a unit sphere metric. Note that the incoming line element, as discussed in [20], can be obtained from the outgoing version by the substitution  $\beta \rightarrow \beta + i\pi/2$ . This fact was used in [6], to obtain a 3D implementation of the incoming null formulation from the one constructed for the outgoing case [10].

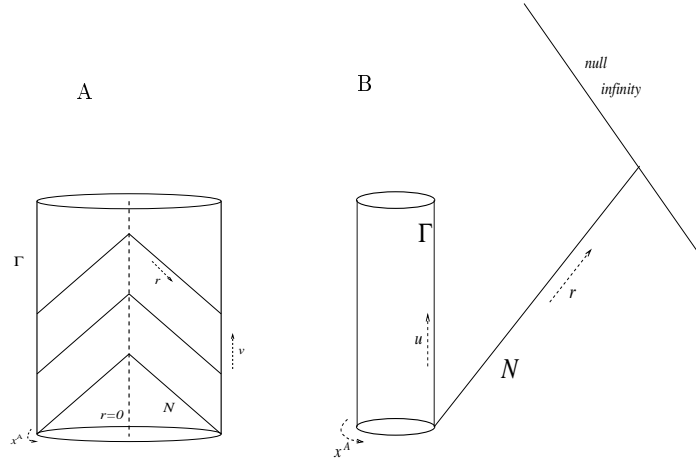


FIG. 1. Incoming (A) and outgoing (B) formulations. In (A), the interior of  $\Gamma$  is covered by a sequence of *incoming* light cones. In (B), the exterior of  $\Gamma$  is covered by a sequence of *outgoing* light cones.

In the spherically symmetric case, Einstein's equations and the evolution equation for the scalar field reduce to:

$$\beta_{,r} = 2\pi r \Phi_{,r}^2, \quad (2.4)$$

$$V_{,r} = -e^{2\beta}, \quad (2.5)$$

$$2(r\Phi)_{,ru} = \frac{1}{r}(rV\Phi_{,r})_{,r}; \quad (2.6)$$

for the outgoing case, while for the incoming one,

$$\tilde{\beta}_{,r} = 2\pi r \tilde{\Phi}_{,r}^2, \quad (2.7)$$

$$\tilde{V}_{,r} = e^{2\tilde{\beta}}, \quad (2.8)$$

$$2(r\tilde{\Phi})_{,ru} = \frac{1}{r}(r\tilde{V}\tilde{\Phi}_{,r})_{,r}, \quad (2.9)$$

(where we distinguish with a tilde the incoming fields from the outgoing ones).

Given that initial data for  $\Phi$  ( $\tilde{\Phi}$ ) on an initial outgoing (incoming) hypersurface and at some worldtube  $\Gamma$  consistent values of  $V$ ,  $\beta$  and  $\Phi$  are provided, the equations can be straightforwardly integrated to yield a unique solution [19,21]. Consistent boundary data on  $\Gamma$  must satisfy constraint equations obtained from  $G_a^r = 8\pi T_a^r$  ( $a = u, x^A$ ).

These conditions are automatically satisfied when matching across  $\Gamma$  to an interior (exterior) solution generated by the incoming (outgoing) evolution [10].

Asymptotic quantities of special interest are the Bondi mass and the scalar news function [22]

$$M(u) = \frac{1}{2}e^{-2H}r^2(V/r)_{,r}|_{r=\infty}, \quad (2.10)$$

$$N(u) = e^{-2H}r\Phi_{,u}|_{r=\infty}; \quad (2.11)$$

where  $H = \beta|_{r=\infty}$ . The Bondi mass loss equation is

$$e^{-2H}M_{,u} = -4\pi N^2 \quad (2.12)$$

This last relation provides an important test to the accuracy of our evolution as

$$M(u = u_o) = M(u = u_f) + 4\pi \int_{u_o}^{u_f} e^{2H} N^2 du, \quad (2.13)$$

which we monitor to assess the validity of our numerical implementation.

### III. MATCHING

Our aim is to match both formulations at a worldtube  $\Gamma$  defined by  $r = R = \text{const}$  (for simplicity, in fact this condition can be relaxed to  $r = R(u)$  and in the 3D case to  $R(u, x^A)$ ). An incoming formulation to be used in the region  $C_i = \{(v, r), r \in [0, R_1]\}$  and an outgoing one in the region  $C_o = \{(u, r), r \in [R_2, \infty)\}$  ( $R_2 < R < R_1$ ). By coupling these codes, consistent boundary values for the outgoing case can be obtained from the incoming variable via a coordinate transformation and viceversa. In the spherical case, obtaining this coordinate transformation is straightforward<sup>‡</sup>. Recall that the incoming line element is given by

$$ds^2 = e^{2\tilde{\beta}} \frac{\tilde{V}}{\tilde{r}} dv^2 + 2e^{2\tilde{\beta}} dv d\tilde{r} + \tilde{r}^2 d\Omega \quad (3.1)$$

Clearly, the transformation

$$dr = d\tilde{r} \quad (3.2)$$

$$du = dv - \tilde{V}/\tilde{r} d\tilde{r} \quad (3.3)$$

takes the incoming formulation into the outgoing one. This transformation is valid everywhere and can be used to obtain boundary values by simply using the transformation law for a 2-tensor field obtaining:

$$e^{\tilde{\beta}} = e^{\beta}, \quad \tilde{V} = -V. \quad (3.4)$$

Additionally, the scalar field must be continuous across  $\Gamma$ , so the condition  $\tilde{\Phi}_\Gamma = \Phi_\Gamma$  applies. Also, in order to ensure “sheet sources” produced by discontinuities in derivatives across  $\Gamma$  will be not be present one might further impose

$$(k^a \nabla_a \tilde{\Phi})^- = (k^a \nabla_a \Phi)^+; \quad (3.5)$$

where the superscripts  $-$  and  $+$  denote the regions to the left and right of  $\Gamma$  respectively and  $k^a$  is an arbitrary vector at the worldtube boundary with non zero radial component.

#### A. Singularity Excision

In order to avoid dealing with singularities, we use excision to remove it from our computational domain. This technique first suggested by Unruh [23] is at present the most successful approach to handle singularities. As it is customary, we excise from the computational domain the region inside an inner trapping boundary defined by the

---

<sup>‡</sup>The matching strategy in the 3D case is naturally more involved and we comment how it can be implemented in the appendix.

following. Given a slice  $S$  on an incoming null hypersurface  $\mathcal{N}$  described in null coordinates by  $r = R(v, x^A)$ , the divergence of the outgoing null normals is given by

$$\begin{aligned} \frac{r^2 e^{2\beta}}{2} \Theta_l = & -V - \frac{1}{\sqrt{q}} [\sqrt{q} (e^{2\beta} h^{AB} R_{,B} - r^2 U^A)],_A \\ & -r (r^{-1} e^{2\beta} h^{AB})_{,r} R_{,A} R_{,B} + r^2 U_{,r}^A R_{,A}. \end{aligned} \quad (3.6)$$

Hence, the slice is marginally trapped if  $\Theta_l = 0$ . In the spherically symmetric case, this reduces to  $r = R(v)$ , and the divergence of the outgoing null rays results

$$F \equiv -2V \frac{e^{-2\beta}}{r^2}, \quad (3.7)$$

Therefore, in our implementation we simply look for the largest  $r = r_e$  for which  $F \leq 0$ ; for  $r < r_e$  the field variables are not integrated and simply set to the values they have at  $r_e$ . This straightforward procedure excises the singularity from the computational domain.

#### IV. NUMERICAL IMPLEMENTATION

We introduce a compactified radial coordinate  $x = r/(1+r)$  (so that  $x = 1 \rightarrow r = \infty$ ). Defining the  $x$  location of the worldtube by  $x_{wt} = R/(1+R)$ , we introduce the outgoing radial grid as  $x_{o_i} = x_{wt} + (i-2)\Delta x_o$  where  $\Delta x_o = (1-x_{wt})/(N_{x_o}-2)$ . Analogously, we define the incoming radial grid as  $x_{i_j} = (j-1)\Delta x_i$  where  $\Delta x_i = x_{wt}/(N_{x_i}-2)$ . Notice that  $x_{o_2} = x_{i_{N_{x_i}-1}} = x_{wt}$ . Hence, there is an overlapping region which will be used to interpolate from one formulation to the other in order to define boundary values. Additionally, we choose  $v = u$  at  $\Gamma$ .

##### A. Evolution Scheme

Integration of the evolution equations is done via the parallelogram approach introduced in [24]. We here describe briefly what this method entails for the outgoing case (it is straightforward to translate it to the incoming case so we do not expand on it). Basically, one recognizes that equation (2.6) is equivalent to

$$2(r\Phi)_{,ur} - \left( \frac{V}{r} (r\Phi)_{,r} \right)_{,r} = - \left( \frac{V}{r} \right)_{,r} \Phi; \quad (4.1)$$

defining  $G = r\Phi$ , the previous equation can be rewritten as

$$\square G = - \left( \frac{V}{r} \right)_{,r} \frac{G}{r}. \quad (4.2)$$

This equation corresponds to the 2-dimensional wave equation in the  $(u, r)$  plane and can be easily integrated over a null parallelogram defined by two sets of outgoing and incoming null geodesics (see figure 2). Hence, the integral identity

$$G_Q = G_P + G_R - G_R + \frac{1}{2} \int_A dudr \left( \frac{V}{r} \right)_{,r} \frac{G}{r}, \quad (4.3)$$

can be used to integrate the scalar field up to global second order accuracy as described in [24]. Additionally, the ‘‘hypersurface’’ equations are discretized by centered second order differences yielding a global second order accurate numerical implementation.

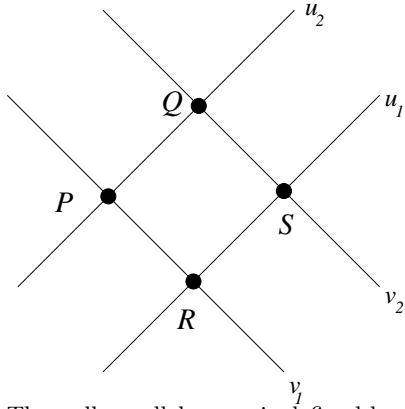


FIG. 2. Parallelogram algorithm set up. The null parallelogram is defined by the intersection of 2 outgoing geodesics with 2 incoming ones.

### B. Matching scheme

A straightforward matching implementation can be obtained by the following scheme. Suppose that at time  $v = u = u_o (= n\Delta u)$  all field variables are known (refer to figure 3). In order to obtain starting values at the level  $v = u = u_o + \Delta u$  one can find the intersection of the incoming null surface at  $v = u_o + \Delta u$  with the outgoing null surface corresponding to  $u = u_o$ , this intersection can be easily obtained in the following way. First, consider the outgoing null ray emanating from  $x_o = (u_o, x_{wt})$  (R in figure 3); the intersection point  $x_i$  of this ray with the incoming one going through at  $u = u_o$  (indicated by S in figure 3) is obtained by requiring that

$$\int_{x_o}^{x_i} ds^2 = 0 \quad (4.4)$$

which implies that  $dr_o = \frac{V}{2r} du$ . Hence, the values of the fields at  $x_i$  can be easily obtained by interpolation of the field on the outgoing patch. This value will be used as starting values to carry out the incoming radial integration. By proceeding in an analogous way one can get values at  $x_o^a = (u_o + \Delta u, R - dr_o)$  (P in figure 3) which provide starting values for the radial integration on the outgoing null surface. Additionally, starting values for the hypersurfaces equations are also obtained by interpolations and applying transformation (3.4).

To ensure continuity of the field and its radial derivatives we proceed as follows. Since the intersection of the null surfaces naturally forms a null parallelogram (see figure 3), one can integrate the evolution equation for  $\Phi$  (as in section 4.1) and obtain the value of  $\Phi_2^{n+1}$  (since the values of  $\Phi$  at all the other corners are either known directly or can be obtained by interpolation from the values of the fields at the previous level). This procedure naturally ensures continuity of the field and its derivative across  $\Gamma$ .

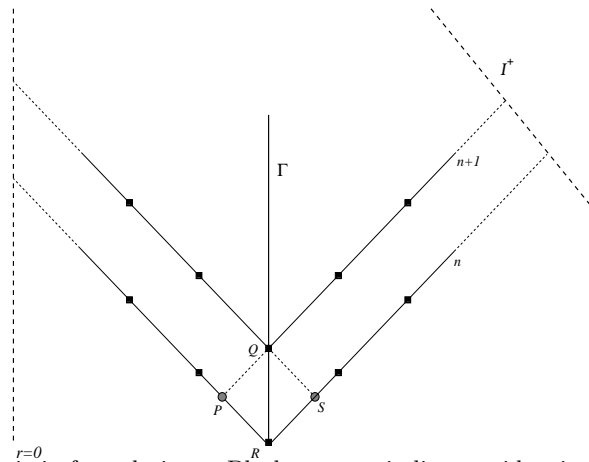


FIG. 3. Matching the characteristic formulations. Black squares indicate grid points while the grey circles indicate the intersection of incoming and outgoing null rays. Points P, Q, R and S define the corners of the parallelogram that will be used for the integration to obtain the value of  $\Phi$  at the  $n + 1$  level on  $\Gamma$ .

## V. TESTS

Our purpose is to present a model demonstrating the feasibility of a stable algorithm based upon two regions that cover the spacetime, where equations are expressed with respect to an incoming or outgoing characteristic formulation. The inner region is evolved using an incoming null algorithm whose inner boundary lies at the apparent horizon (in case it exists, otherwise at  $r = 0$ ) and whose outer boundary  $R_1$  lies beyond the inner boundary of the outer region (located at  $R_2$ ) handled by an outgoing null evolution.

### A. Scalar wave on a flat background

As a first test, we choose initial data corresponding to a scalar wave on a flat background. The initial data for the scalar wave is described by

$$\tilde{\beta} = 0; \tilde{V} = -r; \tilde{\Phi} = 0; \quad (5.1)$$

$$\tilde{\Phi} = \begin{cases} \alpha(1 - r/R_a)^4(1 - r/R_b)^4 & \text{for } r \in [R_a, R_b] \\ 0 & \text{otherwise} \end{cases} \quad (5.2)$$

where the values of  $\beta$  and  $V$  are determined by matching at  $R = 5$  and integrating the hypersurface equations. The value of the field at the origin is chosen so that  $\tilde{\Phi}_{,r} = 0$ . The parameter  $\alpha$  was set to be small enough so that the wave would reach the origin and be dispersed away without a black hole being formed<sup>§</sup>. In our runs, we choose  $R_a = 10, R_b = 20$  and study the system for different values of  $\alpha$  (with  $N_{xi} = N_{xo} = 162$ ). As a test of our numerical implementation we checked that equation (2.13) was satisfied throughout the evolution. Our results for the case  $\alpha = 1$ , are illustrated in figures 4 and 5. Energy conservation is satisfied and the evolution of the scalar field proceeds as expected. The pulse is originally registered at the outgoing patch; as it travels towards the origin it crosses  $\Gamma$ , reaches the origin and it disperses to infinity radiating all the energy contained in the initial data. The spacetime at late times is flat and all the energy of the initial pulse has been radiated away.

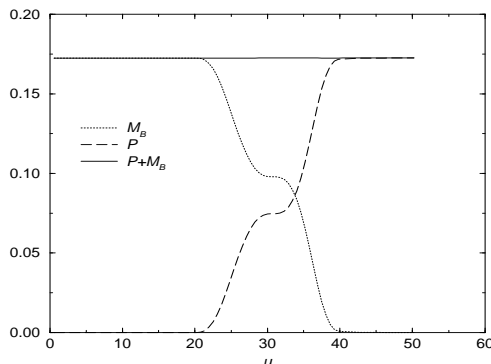


FIG. 4. Conservation of Energy. The plot shows the value of the Bondi mass, the total radiated energy and the addition of the Bondi mass at a given time with the energy radiated until that time (indicated by the solid line). Clearly, the total energy is conserved throughout the evolution.

---

<sup>§</sup>In principle, we could use our numerical implementation to try to look for critical phenomena as first observed by Choptuik [25], we defer such a study to a future work.

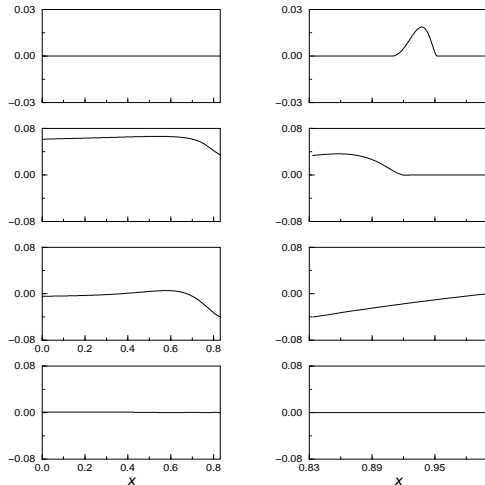


FIG. 5. A sequence of snapshots of the field on both the interior (left) and exterior region (right). From top to bottom the snapshots correspond to  $u = 0, 17, 34$  and  $51$ . Initially the scalar field is non zero only on the exterior region, at later times the field crosses  $\Gamma$ , reaches the origin and it is radiated away to future null infinity leaving behind a flat spacetime.

### B. Collapse of a spherically symmetric scalar wave onto a black hole

We choose initial data corresponding to a Schwarzschild black hole of mass  $M$  which is well separated from a localized pulse of (mostly) incoming scalar radiation. This problem has been thoroughly studied in the past by Marsa and Choptuik [26] in the Cauchy formulation of G.R. Here, we do not try to extend their results, rather, to verify the applicability of  $c^2M$ . Our configuration is such that, initially, there is no scalar field present on the incoming null patch, so the initial data are simply,

$$\tilde{\Phi} = 0, \tilde{\beta} = 0 \quad (5.3)$$

$$\tilde{V} = 2M - \tilde{r}. \quad (5.4)$$

On the outgoing patch we choose  $\Phi$  as a pulse with compact support given by (5.2). The values of  $\beta$  and  $V$  are determined by matching at  $R$  and integrating the hypersurface equations. Inner boundary conditions are not needed since the region inside the marginally trapped surface is excised from the computational domain.

In our tests, we choose  $R = 20M$ ,  $R_a = 40M$ ,  $R_b = 80M$  and again study the evolution of the system for different values of  $\alpha$  (with  $N_{xi} = N_{xo} = 162$ ). As an illustration, we present the results obtained with  $\alpha = 2$ . As shown in figures 6 and 7, the scalar field propagates towards the origin, part of its “original” energy falls into the hole which increases its mass and the rest is radiated away.

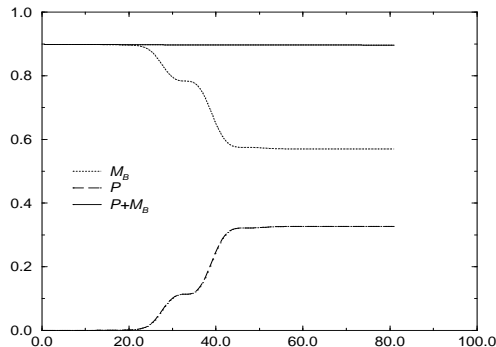


FIG. 6. Conservation of Energy II. The plot shows the value of the Bondi mass, the total radiated energy and the addition of the Bondi mass at a given time with the energy radiated until that time (indicated by the solid line). Values for this run were  $\alpha = 2$ ,  $R_a = 40M$ ,  $R_b = 80M$  and  $R = 20$ . Part of the initial energy contained in the pulse is radiated away while part of it is accreted by the black hole. The final spacetime corresponds to a Schwarzschild spacetime with total mass larger than the initial hole.

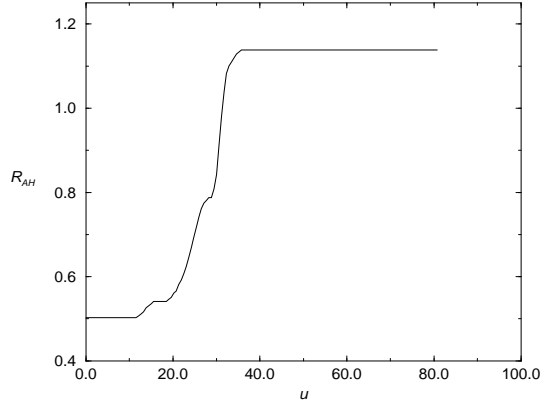


FIG. 7. Apparent horizon location vs. time. The figure shows how the apparent horizon location grows as energy is accreted by the hole. The final asymptotic value of 1.1381 agrees well with twice the value of the Bondi mass at late times ( $2M_B = 1.1388$ ).

The code successfully excises the hole and the area of the apparent horizon reaches an asymptotic value which agrees with twice the value of the Bondi mass at late times (see figure 7). This result fully agrees with what is expected, since at late times the spacetime must be describable by a Schwarzschild metric as a consequence of the no-hair theorems. A sequence of this evolution is illustrated in figure 8.

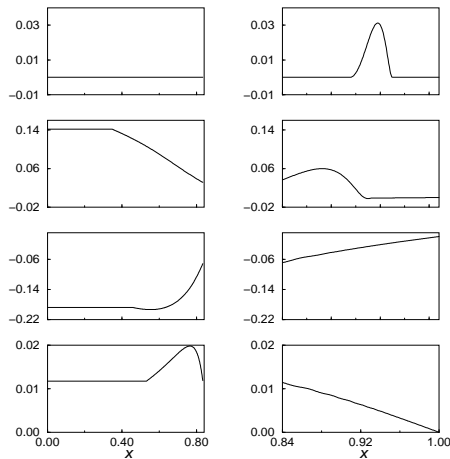


FIG. 8. A sequence of snapshots of the field on both the interior (left) and exterior region (right). From top to bottom the snapshots correspond to  $u = 0, 15, 30$  and  $45$ . Initially the scalar field is non zero only on the exterior region, at later times the field crosses  $\Gamma$ , and reached the black hole which accretes some of the energy and so the masked region increases (shown by the constant lines in the second to fourth plots on the left). The rest is radiated away to future null infinity leaving behind a Schwarzschild spacetime with a larger mass.

Another important test of the algorithm focuses on general aspects of wave propagation in a curved background. The qualitative features of the evolution are well known [27,28]. In particular, a distinctive aspect of wave propagation on curve backgrounds is that Huygens principle does not apply. In a non-flat spacetime, radiation backscatters giving rise to quasinormal modes and tails [29]. Notably, for a given Schwarzschild potential, the power of the late-time tail is characteristic of generic compact support initial data and depends on the multipole structure of it. In particular, at future null infinity the dependence on time goes as  $u^{-2-l}$  (with  $l$  the multipole index). In our case,  $l = 0$  since the initial data corresponds to a spherically symmetric pulse; the value measured from the simulation is  $-2.1$  which agrees with the expected value of  $-2$  (see figure 9). The results obtained here reproduce and, in a way, expand those obtained with Cauchy-characteristic matching [30], as in this case we dynamically find the horizon and use it to excise the hole. The behavior of the apparent horizon location gives a good indication of the energy absorbed by the black hole and its area at late times agrees with that obtained by the asymptotic value of the Bondi mass.



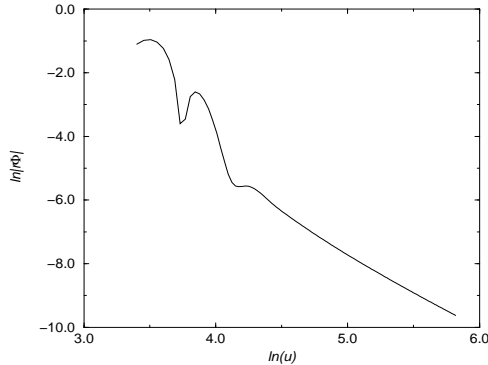


FIG. 9. Late-time power-law tail at null infinity. The measured slope of  $-2.1$  compares well with the theoretical value of  $-2$ .

## VI. PRESENT AND FUTURE OUTLOOK

This work shows that the matching approach of two characteristic formulations provides a way of treating both the inner region and the outer region. At the inner region, it tackles the excision problem as well as other treatments like Cauchy characteristic matching and purely Cauchy or characteristic treatments. It has some advantages over the Cauchy approach because its implementation is much simpler and computationally cheaper. Its disadvantage though, is that it can not be applied in the case where caustics might be present in the integration region. Additionally, it provides a means to reach future null infinity, something that only can be done with the help of a characteristic formulation or the conformal formulation of Einstein’s equations.

This study is the first in a line of research in numerical relativity aiming to fully match characteristic codes to study matter coupled to G.R. Preliminary works have shown that, where applicable, the use of a characteristic evolution can greatly help in investigating this problem. To date however, these studies have been restricted to either the incoming or outgoing formulation, thus not being able to study the inner region or obtaining physical quantities at future null infinity simultaneously. A combination of both approaches appears to be an ideal candidate since it would combine the main advantages of both directions giving access both to future null infinity and to the horizon region in a natural way. Additionally, it might help “avoid” caustics that can be encountered using the single mapping of each formulation. Just as several coordinates patches are necessary to describe nontrivial topologies, a combination of outgoing and incoming coordinates can help to obtain a smooth mapping of the manifold under study. The present work represents the first step towards achieving such a combination. At present,  $3D$  robust implementations exist for both the incoming and outgoing characteristic formulations [10,6]; further, matter treatments studied with these formulations have been successfully implemented [8,9]. Thus, demonstrating the feasibility of combining both approaches in  $1D$  inspired this work. Future studies will address the matter case in  $1D$  (ie. implementing the fluid equations rather than that of a massless scalar field) and proceed with full matching in  $3D$ .

## VII. ACKNOWLEDGEMENTS

This work has been supported by NSF PHY 9800722 and NSF PHY 9800725 to the University of Texas at Austin. The author wishes to thank Pablo Laguna, Jeffrey Winicour, Philipos Papadopoulos and Matthew Choptuik for helpful discussions, Ethan Honda for a careful reading of the manuscript and the National University of Cordoba for its hospitality where part of this work was completed.

## VIII. APPENDIX

A matching strategy for the general  $3D$  case can be devised in a way similar to the one implemented in the Cauchy-characteristic matching approach. In the  $c^2M$  case, however, its application is simpler since no interpolation from a  $3D$  cartesian grid to  $2D$  spheres (slices of the matching worldtube) is required. This matching technique [13] is straightforward. First assume that all field variables are known at hypersurfaces  $\mathcal{N}_v$  and  $\mathcal{N}_{u-\Delta u}$  (and earlier ones); that the matching worldtube is located at  $\tilde{r} = R = \text{const}$  and that  $u = v$  at  $\Gamma$ . The first step which is referred to as *extraction* involves obtaining start-up values (field values at the worldtube) for the outgoing variables at  $\mathcal{N}_u$ . These values are obtained by transforming the incoming metric tensor at  $\mathcal{N}_v$  on  $\Gamma$  to the outgoing coordinate system. Instead of solving the geodesic equation to obtain this coordinate system one can proceed as follows. Choose an “affine” coordinate system  $x^a = (u, \lambda, x^a)$  by

$$x^a = x^a|_{\Gamma} + \lambda l^a + O(\lambda^2) \quad (8.1)$$

where  $x^a|_{\Gamma} = (v, r = R, \tilde{x}^a)$ ;  $l^a$  is an outgoing null vector (normalized by  $l^a dv_a = -1$ ) and we assume the worldtube is at  $\tilde{r} = R = \text{const}$ . By inspection, equation (8.1) is the solution to the geodesic equation with affine parameter  $\lambda$  up to second order in  $\lambda$ . Using this transformation, one can obtain the metric in outgoing null affine coordinates by a simple tensor transformation. The final step requires obtaining  $r$ , as its value can only be known after the angular components of the outgoing null metric are obtained, (refer to [13] for further details). With these values, one can integrate Einstein's equation and completely determine the field values on  $\mathcal{N}_u$ .

The second step, referred to as *injection* requires us to obtain the field values at the intersection of  $\mathcal{N}_{v+\Delta v}$  with  $\mathcal{N}_u$ . This intersection can be obtained up to second order accuracy by means of equation (8.1), since

$$v + \Delta v = v + \lambda l^0|_{\Gamma} + O(\lambda^2), \quad (8.2)$$

$$r_i = R + \lambda l^r|_{\Gamma} + O(\lambda^2). \quad (8.3)$$

From which we can deduce the value of  $r_i$ . Thus, since the values of the fields are known everywhere on  $\mathcal{N}_u$ , we can interpolate to obtain the values of the outgoing fields at the intersection point. Finally, by means of the transformation (8.1), the values of the incoming fields are obtained with which one can integrate the equations inward.

## IX. REFERENCES

- 
- [1] H. Bondi, M. J. G. van der Burg and A. W. K. Metzner, *Proc. R. Soc. Lond. A* **269** (1962) 21.
  - [2] R. Sachs, *Proc. R. Soc. A* **270** (1962) 103.
  - [3] J. Winicour, *Characteristic evolution with matching*, in *Living Reviews* (1998).
  - [4] D. Garfinkle, *Phys. Rev. D* **51** (1995) 5558.
  - [5] R. Hamade and J. Stewart, *Class Quant. Grav.* **13** (1996) 497.
  - [6] R. Gómez, L. Lehner, R. Marsa, and J. Winicour, *Phys. Rev. D* **57** (1997) 4778.
  - [7] The Binary Black Hole Grand Challenge Alliance, *Phys. Rev. Lett.* **80** (1998) 2512.
  - [8] P. Papadopoulos and J. Font gr-qc/9903109 (1999).
  - [9] N. T. Bishop, R. Gómez, L. Lehner, M. Maharaj and J. Winicour, *Phys. Rev. D* **60** (1999) 024005.
  - [10] N. T. Bishop, R. Gómez, L. Lehner, M. Maharaj and J. Winicour, *Phys. Rev. D* **56** (1997) 6298.
  - [11] R. d'Inverno and J. Vickers, *Phys. Rev. D.* **56** (1997) 772.
  - [12] N. Bishop, in *Approaches to Numerical Relativity*, ed. R. d'Inverno (Cambridge UP, Cambridge 1992).
  - [13] N. T. Bishop, R. Gómez, R. A. Isaacson, L. Lehner, B. Szilagyi, and J. Winicour, in *Black Holes, Gravitational Radiation and the Universe*, ed. B. Iyer and B. Bhawal (Kluwer, Dordrecht, 1998).
  - [14] H. Friedrich, *Proc. Roy. Soc. Lond.* **A375** (1981) 169. H. Friedrich, *Proc. Roy. Soc. Lond.* **A378** (1981) 401.
  - [15] P. Huebner, *Class Quant. Grav.* **16** (1999) 2823.
  - [16] J. Frauendiener, *Phys. Rev. D.* **58** (1998) 064003.
  - [17] R. Sachs, *Proc. Roy. Soc. London* **A264** (1961) 309
  - [18] S. Hayward. "Gravitational waves from quasi-spherical black holes", in preparation.
  - [19] D. Christodoulou, *Commun. Math. Phys.* **105** (1986) 337. D. Christodoulou, *Commun. Math. Phys.* **106** (1986) 587.
  - [20] R. Gómez, R. Marsa and J. Winicour, *Phys. Rev. D* **56** (1997) 6310.
  - [21] S. Frittelli and L. Lehner, *Phys. Rev. D* (1999) 084012.
  - [22] R. Gómez R and J. Winicour, *Phys. Rev. D* **48** (1993) 2653.
  - [23] J. Thornburg, *Class and Quantum Grav.* **14** (1987) 1119.
  - [24] R. Gómez, J. Winicour and R. Isaacson, *J. Comp. Phys.* **98** (1992) 11.
  - [25] M. W. Choptuik, *Phys. Rev. Lett.* **70** (1993) 2512.
  - [26] R. Marsa and M. W. Choptuik, *Phys. Rev. D* **54** (1996) 4929.
  - [27] C. Gundlach, R. Price and J. Pullin, *Phys. Rev. D* **49** (1994) 883.
  - [28] E. Ching, P. Leung, W. M. Suen and K. Young, *Phys. Rev. Lett.* **74** (1995) 2414.
  - [29] H. P. Nollert and R. Price, *J.M.P.* **40** (1999) 980.
  - [30] P. Papadopoulos and P. Laguna, *Phys. Rev. D* **55** (1994) 2038.